



The Fourth International Symposium on Innovative Nuclear Energy Systems, INES-4

## Lithium isotope effects upon electrochemical release from lithium manganese oxide

Koji OKANO<sup>a</sup>, Yuta TAKAMI<sup>a</sup>, Satoshi YANASE<sup>a</sup>, Takao OI<sup>a,\*</sup>

<sup>a</sup> Faculty of Science and Technology, Sophia University, 7-1 Kioicho, Chiyodaku, Tokyo, 102-8554 Japan

### Abstract

Lithium was electrochemically released from lithium manganese oxide ( $\text{LiMn}_2\text{O}_4$ ) to an electrolyte solution, a 1:2 v/v mixed solution of ethylene carbonate (EC) and ethylmethyl carbonate (EMC) containing 1 M lithium perchlorate or sodium perchlorate ( $\text{EC/EMC/LiClO}_4$  or  $\text{EC/EMC/NaClO}_4$ ) to observe the lithium isotope effects that accompanied the lithium release. The lighter isotope of lithium,  $^6\text{Li}$ , was preferentially fractionated to the electrolyte solution phase, with the value of the lithium isotope separation factor ranging from 0.989 to 0.971 at 25 °C. The degree of the lithium isotope fractionation was slightly smaller in the  $\text{LiMn}_2\text{O}_4\text{-EC/EMC/NaClO}_4$  system than in the  $\text{LiMn}_2\text{O}_4\text{-EC/EMC/LiClO}_4$  system. The present systems are in great contrast with the lithium cobalt oxide ( $\text{LiCoO}_2$ )-the electrolyte solution systems concerning the direction and magnitude of the lithium isotope effects, which seems mostly ascribable to the structural difference between  $\text{LiMn}_2\text{O}_4$  and  $\text{LiCoO}_2$ .

© 2015 The Authors. Published by Elsevier Ltd. This is an open access article under the CC BY-NC-ND license

(<http://creativecommons.org/licenses/by-nc-nd/3.0/>).

Selection and peer-review under responsibility of the Tokyo Institute of Technology

**Keywords:** lithium isotopes; isotope effects; lithium manganese oxide; separation factor; lithium ion secondary batteries; ethylene carbonate

### 1. Introduction

Naturally occurring lithium consists of two stable isotopes,  $^6\text{Li}$  and  $^7\text{Li}$ .  $^7\text{Li}$  is used as a pH adjustor of coolants of nuclear fission reactors, and  $^6\text{Li}$  is expected to be employed as a blanket material for deuterium-tritium fusion power reactors. Due to these important applications of lithium isotopes, their enrichment and separation has long been studied, and various methods for that purpose have been proposed.

We have been investigating the method of lithium isotope separation based on lithium isotope effects accompanying electrode reactions of lithium ion secondary batteries [1-8]. These reactions may be categorized into

\* Corresponding author. Tel.: +81-3-3238-3359; fax: +81-3-3238-3361.

E-mail address: [t-ooi@sophia.ac.jp](mailto:t-ooi@sophia.ac.jp)

two classes, i. e., the charge and discharge reactions. In charge reactions, lithium atoms or ions in lithium composite oxides cathodes are electrochemically released into an electrolyte solution as lithium ions, and lithium ions in the electrolyte solution are inserted (intercalated) into graphite or other anodes as lithium atoms. In discharge reactions, the reverse phenomena occur. So far, we have investigated only the lithium isotope effects by the charge reaction.

In our previous paper [9], we studied lithium isotope effects accompanying lithium release from the lithium cobalt oxide ( $\text{LiCoO}_2$ ) cathode into an organic electrolyte solution, a 1:2 v/v mixed solution of ethylene carbonate (EC) and ethylmethyl carbonate (EMC) containing 1 M lithium perchlorate ( $\text{LiClO}_4$ ) (EC/EMC/ $\text{LiClO}_4$ ). Lithium cobalt oxide, belonging to the rhombohedral system, is a stable lithium composite oxide with a layered structure and is used as the cathode material in a large majority of lithium ion secondary batteries. The  $^7\text{Li}/^6\text{Li}$  isotopic ratios of the electrodes after the release of 37 to 55% lithium were 1.018 to 1.033 times smaller than that before the release. This means that the heavier isotope,  $^7\text{Li}$ , is preferentially transferred to the electrolyte solution. Contrary to this, the  $^7\text{Li}/^6\text{Li}$  isotopic ratio of the  $\text{LiCoO}_2$  electrode was practically unchanged before and after the 45-62% lithium release into an organic electrolyte solution containing no lithium ions, a 1:2 v/v mixed solution of EC and MEC containing 1 M sodium perchlorate ( $\text{NaClO}_4$ ) (EC/EMC/ $\text{NaClO}_4$ ) [10]. These results indicate that the kind of electrolyte solution is an important factor of determining the direction and the degree of the lithium isotope effects at the cathode-organic electrolyte solution interface. It is of great interest whether this conclusion is general or specific.

In the present work, we studied the lithium isotope effects at the lithium manganese oxide ( $\text{LiMn}_2\text{O}_4$ ) cathode-organic electrolyte solution interface by the charge reaction.  $\text{LiMn}_2\text{O}_4$  with the spinel structure is a compound that is expected to replace  $\text{LiCoO}_2$  as the cathode material in lithium ion secondary batteries owing to the low price of manganese relative to cobalt and the expected higher safety of the  $\text{LiMn}_2\text{O}_4$  electrode [11, 12]. In this paper, we report the results of experiments in which lithium was electrochemically released from the  $\text{LiMn}_2\text{O}_4$  cathode into electrolyte solution and the degree of the lithium isotope effects accompanying the lithium release was measured.

## 2. Experimental

### 2.1. $\text{LiMn}_2\text{O}_4$ cathode and reagents

Fine powders of  $\text{LiMn}_2\text{O}_4$  purchased from Sigma-Aldrich were used as the active cathode material. The lithium manganese oxide cathode was made as follows:  $\text{LiMn}_2\text{O}_4$  powders, a binder and an electro-conductive agent with the weight ratio of 10:1:0.8 were first mixed well to obtain a  $\text{LiMn}_2\text{O}_4$  paste. As the binder, an *N*-methylpyrrolidone (NMP) solution of polyvinylidene fluoride resin (8 wt%) purchased from Kureha Chemical Industry Co. Ltd. was used, and as the electro-conductive agent, a carbon fiber purchased from Showa Denko Co. Ltd. was used. A small amount of NMP was added to the  $\text{LiMn}_2\text{O}_4$  paste, and the resultant mixture was further stirred with a hand mixer for 5 minutes. The  $\text{LiMn}_2\text{O}_4$  slurry thus obtained was manually daubed as uniformly as possible on an electrical current collector, an aluminum foil of 15  $\mu\text{m}$  thick and with a purity of 99.85% purchased from Toyo Aluminium Co. Ltd. The aluminum foil with the slurry on it was heated at 80 °C for 4 hours to remove the NMP component from the slurry to obtain the  $\text{LiMn}_2\text{O}_4$  cathode.

The anode, which consists of a copper foil as an electrical current collector and natural graphite powder coated and pressed on the foil that functions as active material, was manufactured by Piotrek Co. Ltd. Its density, weight and capacity were 1.1  $\text{g}/\text{cm}^3$ , 5.5  $\text{mg}/\text{cm}^2$  and 1.6  $\text{mAh}/\text{cm}^2$ , respectively. Two kinds of EC-based solution, the EC/EMC/ $\text{LiClO}_4$  and EC/EMC/ $\text{NaClO}_4$ , both purchased from Tomiyama Pure Chemical Industry Ltd., were used as the electrolyte solution. The other reagents were of analytical grade and were used without further purification except for hexane, which was used after dehydration with molecular sieves.

### 2.2. Electrochemical release of lithium from the $\text{LiMn}_2\text{O}_4$ cathode into the electrolyte solution

The experimental apparatus used is schematically drawn in Figure 1. It is composed of a power supply (a Hokuto Denko Corp. 201B battery charge/discharge unit), a two-electrode electrochemical cell (electrolytic cell) and a data acquisition unit consisting of an A/D converter and a personal computer (not shown in Figure 1). The volume of the electrolyte solution placed in the cell was 12  $\text{cm}^3$ . The graphite anode and the  $\text{LiMn}_2\text{O}_4$  cathode both with the size of 1 cm times 1 cm, were placed in the face-to-face position in the cell, after reinforced by a stainless steel mesh, so

that the cathode and the anode were wholly immersed in the electrolyte solution. The electrolytic cell was built up in a dry argon atmosphere.

The lithium release from the  $\text{LiMn}_2\text{O}_4$  electrode was performed in the constant current-constant voltage (CC-CV) mode. That is, the electrolysis (lithium release) was at first carried out in the constant current mode (1 mA). As it proceeded, the electric voltage difference between the two electrodes (cell voltage), which was initially about zero, increased and reached the predetermined value of 4.2 or 4.4 V. The electrolytic mode was then automatically changed to the constant voltage mode; the electrolysis was continued and the electric current gradually decreased while keeping the cell voltage at the predetermined value. The electrolysis was continued until the integrated quantity of electricity reached the predetermined value and was discontinued manually. The temperature of the electrolytic cell was kept constant at 25 °C throughout the electrolysis.

### 2.3. Analyses and measurements

After the electrolysis was over, the cathode was taken out of the electrolytic cell in a dry argon atmosphere, washed with dehydrated hexane and was allowed to stand for hours to remove adhering hexane by evaporation. The lithium-released  $\text{LiMn}_2\text{O}_4$  was recovered from the aluminum foil and heated at 700 °C for 3 h. The resultant lithium manganese composite oxides was dissolved with 6 M hydrochloric acid, and the lithium and manganese concentrations in the solution thus obtained was measured to obtain the amounts of lithium and manganese in the cathode after the lithium release. The amounts of the metals before the electrolytic experiment were determined in a similar way using the virgin cathode.

The sample preparation for the mass spectrometric analysis for the  $^7\text{Li}/^6\text{Li}$  isotopic ratio of the cathode was carried out as follows: A part of the lithium and manganese-dissolved hydrochloric solution was first evaporated to dryness. The evaporation residue was dissolved with distilled water, and the resultant solution was passed through a cation exchange column in the hydrogen form. Lithium ions trapped on the column were eluted out with 0.5 M hydrochloric acid while manganese ions stayed on the column. The former ions were thus separated from the latter ions. Lithium chloride from the cation exchange column was converted to lithium hydroxide through anion exchange and further converted to lithium iodide by the reaction with hydroiodic acid. The lithium iodide thus prepared was subjected to the mass spectrometric analysis for the  $^7\text{Li}/^6\text{Li}$  isotopic ratio.

After the electrolysis was finished, the anode was taken out of the cell in a dry argon atmosphere, washed with dehydrated hexane and was allowed to stand for hours to remove adhering hexane by evaporation. The lithium-and/or sodium-inserted graphite was recovered from the copper foil and immersed in 0.1 M HCl overnight in order to stoichiometrically extract the inserted lithium and sodium. The amounts of lithium and sodium inserted in the graphite anode were calculated by measuring the concentrations of lithium and sodium in the HCl solution thus obtained.

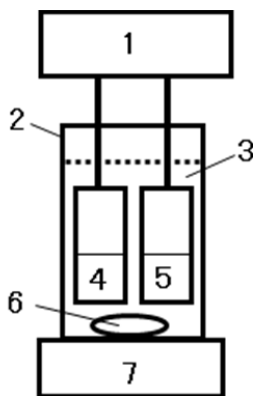


Fig. 1. The experimental apparatus. 1, charge-discharge controller (power supply); 2, electrolytic cell; 3, electrolyte solution; 4,  $\text{LiMn}_2\text{O}_4$  cathode; 5, graphite anode; 6, stirrer tip; 7, magnetic stirrer

An aliquot of the EC/EMC/NaClO<sub>4</sub> after the electrolysis was evaporated to dryness to remove the solvent (EC and EMC). The evaporation residue, which was basically a mixture of sodium and lithium perchlorates, was dissolved with distilled water. The obtained solution was added to a chromatographic quartz column (30 cm in length and 2 cm $\phi$  in diameter), in which a cation exchange resin in the hydrogen form (Muromac 50W-X8, 200-400 mesh) was packed, and eluted with 0.5 M HCl to separate lithium from sodium [13]. The resin column height was 25.0 cm and the flow rate of the eluent was 4 cm<sup>3</sup>·min<sup>-1</sup>. The 200-350 cm<sup>3</sup> portion of the effluent which contained lithium ions but not sodium ions was collected. The lithium recovery was 96% or better. A part of the purified lithium from the EC/EMC/NaClO<sub>4</sub> was used for the determination of the amount of the lithium released to the electrolyte solution and the remaining was subjected to the mass spectrometric analysis after the conversion to lithium iodide.

Concentrations of lithium and sodium in aqueous solutions were measured by flame photometry with a Thermo Electron SOLAAR M mkII atomic adsorption spectrometer, and that of manganese by inductively coupled plasma-atomic emission spectroscopy (ICP-AES) with a Seiko Instruments SPS7700 ICP-AES spectrometer, respectively. The powder X-ray diffraction (XRD) patterns of LiMn<sub>2</sub>O<sub>4</sub> samples were recorded using a Rigaku RINT 2100 V/P X-ray diffractometer with Cu K $\alpha$  radiation in the 2 $\theta$  range of 5-80° at room temperature. Scanning electron microscopy (SEM) photographs were taken with a Hitachi SU-8000 electron microscope. The <sup>7</sup>Li/<sup>6</sup>Li isotopic ratios of the samples were determined by the surface ionization technique with a Finnigan MAT 261 mass spectrometer. The details of the <sup>7</sup>Li/<sup>6</sup>Li isotopic ratio measurements were found in our previous paper [14].

#### 2.4. Lithium isotopic data treatment

The magnitude of the lithium isotope effects upon electrochemical release from LiMn<sub>2</sub>O<sub>4</sub> to the electrolyte solution (EC/EMC/NaClO<sub>4</sub> or EC/EMC/LiClO<sub>4</sub>) was evaluated by the following three factors.

The lithium isotopic variation factor,  $R$ , is defined as

$$R = ({}^7\text{Li}/{}^6\text{Li})_{\text{B-cathode}} / ({}^7\text{Li}/{}^6\text{Li})_{\text{A-cathode}} \quad (1)$$

where  $({}^7\text{Li}/{}^6\text{Li})_{\text{A-cathode}}$  denotes the <sup>7</sup>Li/<sup>6</sup>Li isotopic ratio of lithium in the cathode after the lithium release and  $({}^7\text{Li}/{}^6\text{Li})_{\text{B-cathode}}$  denotes that before the lithium release. Both  $({}^7\text{Li}/{}^6\text{Li})_{\text{A-cathode}}$  and  $({}^7\text{Li}/{}^6\text{Li})_{\text{B-cathode}}$  are experimentally determined quantities.

The observed lithium isotope separation factor,  $S$ , is defined as

$$S = ({}^7\text{Li}/{}^6\text{Li})_{\text{A-electrolyte(obs)}} / ({}^7\text{Li}/{}^6\text{Li})_{\text{A-cathode}} \quad (2)$$

where  $({}^7\text{Li}/{}^6\text{Li})_{\text{A-electrolyte(obs)}}$  is the measured isotopic ratio of the lithium released to the electrolyte solution. Both  $({}^7\text{Li}/{}^6\text{Li})_{\text{A-electrolyte(obs)}}$  and  $({}^7\text{Li}/{}^6\text{Li})_{\text{A-cathode}}$  are experimentally determined quantities. For experiments with the EC/EMC/NaClO<sub>4</sub>, the <sup>7</sup>Li/<sup>6</sup>Li ratio of the lithium released to the electrolyte solution was measured; this was impossible for the LiMn<sub>2</sub>O<sub>4</sub>- EC/EMC/LiClO<sub>4</sub> (Mn-Li) system.

The estimated lithium isotope separation factor,  $S^*$ , is defined as

$$S^* = ({}^7\text{Li}/{}^6\text{Li})_{\text{A-electrolyte(calc)}} / ({}^7\text{Li}/{}^6\text{Li})_{\text{A-cathode}} \quad (3)$$

where  $({}^7\text{Li}/{}^6\text{Li})_{\text{A-electrolyte(calc)}}$  is the lithium isotopic ratio of the released lithium calculated using  $({}^7\text{Li}/{}^6\text{Li})_{\text{B-cathode}}$ ,  $({}^7\text{Li}/{}^6\text{Li})_{\text{A-cathode}}$  and the amounts of lithium in the cathode before and after the lithium release.

The quantities  $S$  and  $S^*$  are the measures of the lithium isotope effects occurring at the LiMn<sub>2</sub>O<sub>4</sub> cathode–EC/EMC/LiClO<sub>4</sub> and LiMn<sub>2</sub>O<sub>4</sub> cathode–EC/EMC/NaClO<sub>4</sub> interfaces. If every analysis is completely accurate, the value of  $S^*$  should agree with that of  $S$ . By definition,  $R$ ,  $S$  and  $S^*$  are all larger than unity when the heavier isotope of lithium is preferentially fractionated to the electrolyte solution phase.

### 3. Results and discussion

A SEM photograph of a virgin cathode is shown in Figure 2. It is seen that the grain size of  $\text{LiMn}_2\text{O}_4$  particles is roughly from 50 nm to 1  $\mu\text{m}$ . The string-like substances are carbon fibers used as the electro-conductive agent. An XRD pattern of a cathode after the electrolysis with the estimated degree of lithium release of about 40% is shown in Figure 3. The main phase of  $\text{Li}_{1-x}\text{Mn}_2\text{O}_4$  [15] is maintained even after the lithium release with two unknown peaks at about  $2\theta$  of 21 and  $24^\circ$ .

In the present experiments, the reaction occurring at the cathode is expressed as



At the anode, the cation ( $\text{Li}^+$ ,  $\text{Na}^+$ ) is inserted in graphite,



Experimental conditions and results are summarized in Table 1. Two series of experiments were carried out. In one series of experiments (Mn-Li system), the EC/EMC/ $\text{LiClO}_4$  was used as the electrolyte solution, and in the other series ( $\text{LiMn}_2\text{O}_4$ -EC/EMC/ $\text{NaClO}_4$  (Mn-Na) system), the EC/EMC/ $\text{NaClO}_4$  was used as the electrolyte solution.

Table 1. Summary of experimental conditions and results									
Run No.	Salt in the electrolyte solution	Electrolysis time (sec)	Integrated quantity of electricity (C)	Li/Mn ratio after Li release	Proportion of Li released (%)	Current efficiency (%)	R	S	S'
L-01	$\text{LiClO}_4$	6640	2.07	0.360	32	36	0.992		0.974
L-02	$\text{LiClO}_4$	9300	3.27	0.290	45	33	0.992		0.982
L-03	$\text{LiClO}_4$	19100	3.90	0.378	28	61	0.991		0.971
N-01	$\text{NaClO}_4$	7040	3.67	0.231	56	82	0.995	0.989	0.991
N-02	$\text{NaClO}_4$	14500	4.16	0.210	61	62	0.991	0.985	0.983
N-03	$\text{NaClO}_4$	18000	4.26	0.135	75	65	0.984	0.977	0.978
Temperature: 25 °C, solvent: EC/EMC, Li/Mn ratio of virgin electrode: 0.527.									
Predetermined cell voltage: 4.2 V (for L-02, 4.4 V), predetermined electric current: 1 mA.									

The electrolysis time was varied from 6640 to 19100 s and the integrated quantity of electricity ranged from 2.07 to 4.26 C. Comparing at a similar electrolysis time, the integrated quantity of electricity tends to be larger for the Mn-Na system than for the Mn-Li system. This indicates that the former is a better electrolyte solution than the latter as far as time required for attaining the predetermined integrated quantity of electricity. An example of the changes of the cell voltage and the electric current during an electrolytic course (Run L-02) is shown in Figure 4. The cell voltage increased very quickly from the initial value of about zero at the beginning of the electrolysis and then gradually approached the predetermined value of 4.4 V. After 1026 s from the commencement of the electrolysis, it reached the predetermined value and was kept constant thereafter. The electric current was kept constant at 1 mA until the cell voltage reached the predetermined value and then started decreasing with the rate of decrease being large at first and becoming gradually small.

The mole ratio of lithium to manganese, Li/Mn, of the virgin  $\text{LiMn}_2\text{O}_4$  material was found to be 0.527, slightly larger than the theoretical value of 0.5. This ratio became 0.135 to 0.378 after the electrolysis, which clearly shows that part of lithium was transferred from the cathode to the electrolyte solution by the charge reaction. The proportion of lithium released to the electrolyte solution was estimated to range from 0.28 (28%) to 0.75 (75%). No release of manganese ion was observed.

The electric current efficiency (%), which is defined as 100 times the ratio of the amount of the released lithium to the amount that corresponds to the integrated quantity of electricity, ranged from 33 to 82%. Other than the experimental errors, a possible reason for the current efficiency less than 100% may be an insufficient hexane washing of the electrode after the electrolysis; a small portion of lithium ions in the electrolyte solution may have survived the hexane washing and have kept confined in small pores formed at grain boundaries on the surface of the

electrode, which certainly contributed to reducing the current efficiency. A SEM photograph of the surface of a cathode after the electrolysis is shown in Figure 5. Sphere-shaped substances, which we consider as small drops of the electrolyte solution confined in a pore on the electrode surface, are observed. The current efficiency of the Mn-Li system was lower, ranging from 33 to 61%, than that of the Mn-Na system, ranging from 62 to 82%. This difference in the current efficiency may be attributable to the fact that concentrations of lithium were much higher in the former than in the latter, and consequently, the degree of the contamination of the cathode by the adhering electrolyte solution is expected to be larger for the former.

### 3.1. Lithium isotope effects

The values of  $R$ ,  $S$  and  $S'$  are summarized in the last three columns of Table 1. They are all smaller than unity, which means that the lighter isotope,  ${}^6\text{Li}$ , is preferentially fractionated in the electrolyte solution and the cathode is enriched in the heavier isotope,  ${}^7\text{Li}$ , after the lithium release in every experiment. For the Mn-Na system, both  $S$  and  $S'$  are calculated and they are very similar to each other in every experiment, which indicates the satisfactorily high accuracy of the present chemical analyses including the mass spectrometric measurements of the lithium isotopic ratios.

The value of  $S'$  ranges from 0.971 to 0.982 for the Mn-Li system. It is in great contrast with the  $\text{LiCoO}_2\text{-EC/EMC/LiClO}_4$  (Co-Li) system in our previous paper [9] in which lithium was electrochemically released from the  $\text{LiCoO}_2$  electrode to the EC/EMC/LiClO<sub>4</sub>, and accompanying the release, substantial depletion of  ${}^7\text{Li}$  was observed on the cathode after the electrolysis with the value of  $S'$  (expressed as  $S$  in [9]) ranging from 1.045 to 1.060. The two systems give just the opposite lithium isotope effects. In the previous paper [9], we explained the lithium isotope fractionation observed in the Co-Li system based on the equilibrium lithium isotope effects between lithium remaining in the  $\text{LiCoO}_2$  and lithium released to the electrolyte solution. That is, we considered that the observed lithium isotope fractionation originated from the fact that the equilibrium constant of the lithium isotope exchange reaction,



where  ${}^i\text{Li}_{\text{A-cathode}}$  denotes lithium- $i$  ( $i = 6$  or  $7$ ) in the  $\text{LiCoO}_2$  phase and  ${}^i\text{Li}_{\text{A-electrolyte}}$  denotes lithium- $i$  released to the electrolyte solution phase, is larger than unity.  $\text{LiCoO}_2$  has a laminated structure in which lithium atoms are located between layers formed by cobalt and oxide ions and are mobile in close-packed oxygen arrays [16,17]. It is thus highly probable that lithium atoms are more loosely bound in  $\text{LiCoO}_2$  than lithium ions in the EC/EMC/LiClO<sub>4</sub> in which they are solvated by four EC molecules [18]. Based on the theory of equilibrium isotope effects [19], the heavier isotope is preferentially fractionated into the more stiffly bound state. That is,  ${}^7\text{Li}$  is expected to be enriched in the electrolyte solution phase with the equilibrium constant of Eq. (6) being larger than unity, which agrees with the experimental results in a qualitative fashion.



Fig. 2. A SEM photograph of the surface of a virgin  $\text{LiMn}_2\text{O}_4$  cathode

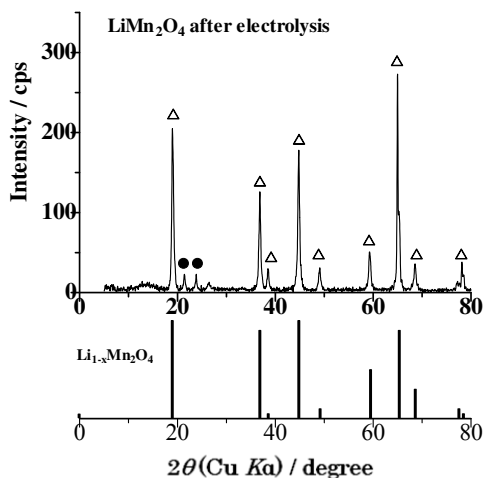


Fig. 3. An XRD pattern of a  $\text{LiMn}_2\text{O}_4$  cathode after the electrolysis. Triangles,  $\text{LiMn}_2\text{O}_4$ ; circles, unknown. The reference pattern of  $\text{Li}_{1-x}\text{Mn}_2\text{O}_4$  is cited from Thackeray et al. (1983).

A similar explanation may be applied to the present Mn-Li system.  $\text{LiMn}_2\text{O}_4$  has a spinel structure; oxide ions form the face-centered cubic lattice and a lithium ion is located at the center of a tetrahedron formed by four oxide ions [15, 20]. Thus, the lithium ion is considered to be tightly constrained in the spinel structure, more tightly than the lithium ion in the EC/EMC/ $\text{LiClO}_4$ , which leads to the preferential fractionation of the heavier isotope of lithium into the  $\text{LiMn}_2\text{O}_4$  phase.

As mentioned above, the lithium ion in  $\text{LiMn}_2\text{O}_4$  must be more stiffly bound than the lithium atom in  $\text{LiCoO}_2$  in order to explain the directions of the lithium isotope effects observed in the Mn-Li and Co-Li systems. Supporting evidence is found in the Li-O bond distances in the two crystals. The Li-O distance in  $\text{LiMn}_2\text{O}_4$  is 1.967 Å while that in  $\text{LiCoO}_2$  is 2.093 Å [21, 22]. A shorter bond distance is an indicator of stiffer bound state. A more persuasive support would be to show that the value of lithium isotopic reduced partition function ratios (RPFs) is in the sequence of  $\text{LiMn}_2\text{O}_4 > \text{EC/EMC/LiClO}_4 > \text{LiCoO}_2$ . So far, calculations of RPFs of lithium in crystals are unsuccessful, and such calculations are certainly one of our future targets.

For the Mn-Na system, the value of  $S$  ranges from 0.977 to 0.989, slightly larger (closer to unity) than that for the Mn-Li system. That is, the direction of the isotope fractionation in the Mn-Na system is the same as that of the Mn-Li system, but the degree of the isotope fractionation is smaller in the former than in the latter. These findings are explainable as a partial manifestation of the equilibrium isotope effects based on Eq. (6) as in the case of the lithium isotope effects with  $\text{LiCoO}_2$  electrodes, although the direction of the effects is just opposite in the two systems [10]. At the early stage of the electrolysis in the Mn-Na system, lithium ions released from the cathode will diffuse promptly into the whole solvent, which is not accompanied by any lithium isotope effects. In the latter part of the electrolytic course, however, the concentration of lithium in the electrolyte solution gradually increases especially near the  $\text{LiMn}_2\text{O}_4$  cathode-EC/EMC/ $\text{NaClO}_4$  interface, and the lithium isotopic equilibrium is attained between the cathode and the electrolyte solution, which leads to the preferential fractionation of the lighter isotope of lithium in the electrolyte solution phase. In the Mn-Na system, the magnitude of the deviation of the value of  $S$  from unity is an increasing function of the proportion of the released lithium (Table 1), which seems to support this speculation.

The above explanation for the lithium isotope effects observed in the present work is based on the equilibrium isotope effects [19]. The explanation based on the kinetic isotope effects [23] may also be possible and more straightforward. The reaction rate of the lighter isotope is in general larger than that of the heavier counterpart. In the present case, the lighter isotope of lithium transferred faster from the cathode to the electrolyte solution, which leads to the preferential fractionation of  $^6\text{Li}$  in the electrolyte solution phase, giving the value of separation factor smaller

than unity. This explanation, however, cannot be applied to the results of the experiments with the  $\text{LiCoO}_2$  cathode. The explanation based on the equilibrium isotope effects seems more generally applied. At the present stage of the progress of our study on the lithium isotope effects at the cathode/electrolyte solution interface by the charge reaction, however, it is difficult to draw a decisive conclusion on what is the origin of the observed lithium isotope fractionation; equilibrium or kinetic isotope effects or their combination. We need to accumulate more experimental data, and, towards that direction, we have already started the work to observe lithium isotope effects by the charge reaction using such potential electrode materials as lithium iron phosphate and lithium nickel oxide.

#### 4. Conclusion

To summarize the present study, we make the following statements.

Our handmade  $\text{LiMn}_2\text{O}_4$  electrode functioned as the cathode in an apparatus mimicking lithium ion secondary batteries as far as the first charging is concerned. By the charge reaction, 32 to 75% of lithium in the cathode was released to the electrolyte solution, whereas no release of manganese was observed.

Lithium isotope effects were observed upon the electrochemical release of lithium from the  $\text{LiMn}_2\text{O}_4$  electrode to the electrolyte solution, an EC/EMC mixed solution containing 1 M  $\text{LiClO}_4$  or  $\text{NaClO}_4$ . The lighter isotope of lithium was preferentially fractionated to the electrolyte solution phase with the value of the isotope separation factor ranging from 0.971 to 0.989 at 25 °C. These results are in marked contrast with experiments with the  $\text{LiCoO}_2$  electrode [9, 10] and seem ascribable mostly to the structural difference between  $\text{LiMn}_2\text{O}_4$  and  $\text{LiCoO}_2$ .

#### Acknowledgements

We acknowledge Dr. M. Nomura, Tokyo Institute of Technology, for his assistance in mass spectrometric measurements of lithium isotopic ratios. This work was supported in part by a Grant-in-Aid (No. 23561015) from the Ministry of Education, Culture, Sports, Science, and Technology.

#### References

- [1] Yanase S, Oi T, Hashikawa S. Observation of lithium isotope effect accompanying electrochemical insertion of lithium into tin. *J Nucl Sci Technol* 2000; 37: 919-923.
- [2] Yanase S, Hayama W, Oi T. Lithium isotope effect accompanying electrochemical intercalation of lithium into graphite. *Z Naturforsch* 2003; 58a:306–312.
- [3] Hashikawa S, Yanase S, Oi T. Observation of lithium isotope effect accompanying chemical insertion of lithium into graphite. *Z Naturforsch* 2002; 57a:857–862.
- [4] Mouri M, Asano K, Yanase S, T. Oi. Lithium isotope effects accompanying electrochemical insertion of lithium into metal oxides. *J Nucl Sci Technol* 2007; 44:73–80.

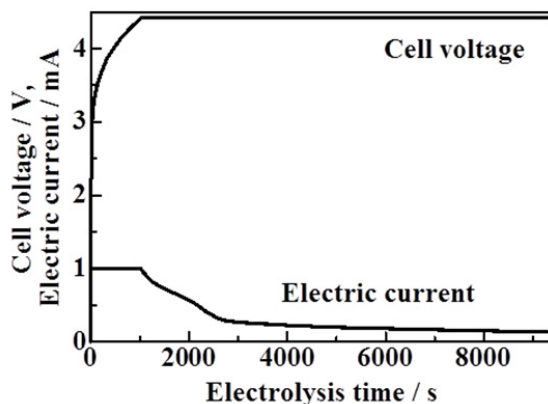


Fig. 4. Changes of the cell voltage and electric current with the passage of the electrolysis time of Run L-02.



- [5] Mouri M, Yanase S, T. Oi. Observation of lithium isotope effects accompanying electrochemical insertion of lithium into zinc. *J Nucl Sci Technol* 2008; 45:384–389.
- [6] Asano K, Yanase S, T. Oi. Lithium isotope effect accompanying electrochemical insertion of lithium into Tin(IV) sulfide. *J Nucl Sci Technol Supplement* 52008; 24–29.
- [7] Zenzai K, Yanase S, Zhang YH, Oi T. Lithium isotope effect accompanying electrochemical insertion of lithium into gallium. *Prog Nucl Energy* 2008; 50:494–498.
- [8] Saito S, S., Takami Y, Yoshizawa-Fujita M, Yanase S, Oi T. Lithium isotope effects upon electrochemical lithium insertion to host material from ionic liquid medium. *Prog Nucl Energy* 2011; 53:999-1004.
- [9] Takami Y, Yanase S, Oi T. Observation of lithium isotope effects accompanying electrochemical release from lithium cobalt oxide. *Z Naturforsch A* 2013; 68a:3-78.
- [10] Takami Y, Yanase S, Oi T. Lithium isotope effects upon electrochemical release from lithium cobalt oxide to non-lithium electrolyte solution, *Z Naturforsch A* 2014; 69a:97-103.
- [11] Kano G, Takeuchi Y, Nishimuta Y, Furuichi Y, Takashima M, Synthesis and lithium secondary battery characteristics of spinel  $\text{LiMn}_2\text{O}_4$ . *Shigen Shori Gijyutsu (Resources Processing)* 1995; 42:99-103 (in Japanese).
- [12] Ling GW, Zhu X, He YB, Song QS, Li B, Li YJ, Yang QH, Tang ZY. Structural and thermal stabilities of spinel  $\text{LiMn}_2\text{O}_4$  materials under commercial power batteries cycling and abusive conditions. *Int J Electrochem Sci* 2012; 7:2455-2467.
- [13] Oi T, Odagiri T, Nomura N. Extraction of lithium from GSJ rock reference samples and determination of their lithium isotopic compositions. *Anal Chim Acta* 1997; 340:221-225.
- [14] Oi T, Kawada K, Hosoe M, Kakihana H. Fractionation of lithium isotopes in cation-exchange chromatography. *Sep Sci Technol* 1991; 26:1353–1375.
- [15] Thackeray MM, David WIF, Bruce PG, Goodenough JB. Lithium insertion into manganese spinels. *Mater Res Bull* 1983; 18:461-472.
- [16] Mizushima K, Jones PC, Wiseman PJ, Goodenough JB.  $\text{Li}_x\text{CoO}_2$  ( $0 < x \leq 1$ ): a new cathode material for batteries of high energy density. *Mat Res Bull* 1980; 15:783-789.
- [17] Mizushima K, Jones PC, Wiseman PJ, Goodenough JB.  $\text{Li}_x\text{CoO}_2$  ( $0 < x \leq 1$ ): a new cathode material for batteries of high energy density. *Solid State Ionics* 1981; 3/4:171-174.
- [18] Yanase S, Oi T. Solvation of lithium ion in organic electrolyte solutions and its isotopic reduced partition function ratio studied by *ab initio* molecular orbital method. *J Nucl Sci Technol* 2002; 39:1060-1064.
- [19] Bigeleisen J, Mayer MG. Calculation of equilibrium constants for isotopic exchange reactions. *J Chem Phys* 1947; 15:261-267.
- [20] Yu ZM, Zhao LC. Structure and electrochemical properties of  $\text{LiMn}_2\text{O}_4$ . *Trans Nonferrous Met Soc China* 2007; 17:659-664.
- [21] Rodríguez-Carvajal J, Rousse G, Masquelier C, Hervieu M. Electronic crystallization in a lithium battery materials: Columnar ordering of electrons and holes in the spinel  $\text{LiNi}_2\text{O}_4$ . *Phys Rev Lett* 1998; 81:4660-4993.
- [22] Akimoto J, Gotoh Y, Oosawa Y. Synthesis and structure refinement of  $\text{LiCoO}_2$  single crystals. *J Solid State Chem* 1998; 141:298-302.
- [23] Van Hook WA. Kinetic isotope effects: Introduction and discussion of the theory. in: Collins CJ, Bowman NS, editors. *Isotope effects in chemical reactions*, ACS monograph 167. New York: Van Nostrand Reinhold Company; 1970. p. 1-89.